Z-PINNING APPROACH FOR IMPROVING INTERLAYER STRENGTH OF 3D PRINTED PARTS

Chad Duty[1,2], Jordan Failla[1,2], Seokpum Kim[2], Tyler Smith[1,2], John Lindahl[2], Alexander Lambert[2], Vlastimil Kunc[1-3]

[1]University of Tennessee
Knoxville, TN

[2]Manufacturing Demonstration Facility
Oak Ridge National Laboratory
Oak Ridge, TN

[3]Purdue University
West Lafayette, IN

ABSTRACT

Since additively manufactured (AM) parts are built in a layer-wise fashion, the mechanical properties are typically highly anisotropic. Extrusion-based AM systems like fused filament fabrication (FFF) commonly demonstrate a 50-75 % decrease in mechanical strength in the build direction (z-axis) compared to the x-y plane. This study presents a novel 3D printing approach called "z-pinning" that allows deposition of material across build layers throughout the volume of the part. Initial results with polylactic acid (PLA) and carbon fiber reinforced PLA have shown an increase in the z-direction strength by a factor of 3.5x. Direct comparison with x-direction strength for z-pinned samples also demonstrated a significant reduction in mechanical anisotropy – with some samples showing a quasi-isotropic response.

1. INTRODUCTION

Extrusion deposition additive manufacturing (EDAM) techniques, such as fused filament fabrication (FFF), build up three-dimensional objects by depositing material in a two-dimensional layer that is added onto previously deposited layers in a successive fashion. Although this layer-based approach can produce very complex geometries, the internal structure of the part places an inherent limitation on the mechanical performance. Since FFF technologies only deposit continuous material in the build plane (conventionally labeled the x-y plane), the transmission of forces in the build direction (the z-axis) must rely on the interfacial strength between successively deposited layers. Several researchers have documented the mechanical anisotropy typically found in EDAM parts, spanning multiple materials and size scales. For two of the most common FFF thermoplastics, acrylonitrile butadiene styrene (ABS) and polylactic

This manuscript has been authored in part by UT-Battelle, LLC under Contract No. DE-AC05-00OR22725 with the U.S. Department of Energy. The United States Government retains and the publisher, by accepting the article for publication, acknowledges that the United States Government retains a non-exclusive, paid-up, irrevocable, world-wide license to publish or reproduce the published form of this manuscript, or allow others to do so, for United States Government purposes. The Department of Energy will provide public access to these results of federally sponsored research in accordance with the DOE Public Access Plan (http://energy.gov/downloads/doe-public-access-plan).

SAMPE Conference Proceedings. Charlotte, NC, May 20-23, 2019. Society for the Advancement of Material and Process Engineering – North America.

acid (PLA), the ultimate tensile strength across build layers (z-direction) is typically 33 % to 80 % lower than the corresponding strength along the primary axis of deposition (x-direction) [1-4]. Similar studies with fiber reinforced materials (ABS and PLA matrix) demonstrate a reduction in strength ranging from 33 % up to 97 % [1, 2, 4, 5]. Large scale EDAM systems also produce components that demonstrate similar trends for both neat and reinforced materials, reductions ranging from 25 % to 90 % [6, 7].

1.1 Mitigation efforts

There have been numerous efforts to improve the inter-layer strength of EDAM components and thereby reduce the mechanical anisotropy. Since the inter-layer bond strength of EDAM parts is attributed to the degree of interdiffusion of polymer chains across the interface [8-10], several approaches have focused on increasing the amount of time that the bond surface stays above the glass transition temperature. In-situ heating techniques have been explored that use radiant sources [11-13] or forced convection [14] to improve z-direction properties by 50-100 %. Some post-process approaches have also shown potential, using either radiation [3] or microwave energy [15] to increase z-direction performance by 50-275 %.

More recently, some research efforts have attempted to deposit continuous material out of the traditional x-y plane to produce curved structures [16] or to intentionally align the principal stresses within the component to the "strong" direction of the printed material [17, 18]. Others have shown that printing an oriented "skin" on the outer surface of a traditionally printed part can increase the z-direction strength by ~50 % [19, 20].

1.2 Z-Pinning Approach

The current paper focuses on a z-pinning approach for EDAM structures that allows the deposition of continuous material across build layers (in the z-direction) throughout the volume of a part. Figure 1 illustrates the z-pinning process. Initially (Fig 1a), a structure is deposited in a conventional fashion that includes intentionally-aligned holes in the x-y plane. After a certain number of layers (*n*) have been completed, the printer head is positioned over one of the holes and material is extruded in z-direction to fill the hole (Fig 1b). The remaining hole in the structure is left open and additional (*n*) layers are added while maintaining the aligned voids in the structure (Fig 1c). The printer head is then positioned over the alternate hole and material is extruded to create a "z-pin" of length *2n* (Fig 1d). The pattern continues as the structure grows and additional "*2n*-long" pins are deposited in alternating locations (Figs 1e-f).

Alternating the x-y location of deposited pins allows for staggering of the "seam" between stacked pins. In the illustration of Figure 1, pins that are four layers long are deposited in alternating locations every two layers. The naming convention for this type of "A/B" pin configuration is "4-2" pins. An alternate "A/B/C" configuration could deposit pins that were six layers long every two layers. In this case, the "6-2" pins would only fill one-third of the available holes in each layer and the seams between adjacent pins would be separated by two layers. If additional distance between the seams were desired, an "A/B" configuration of "6-3" pins could be considered (or any other reasonable variation).

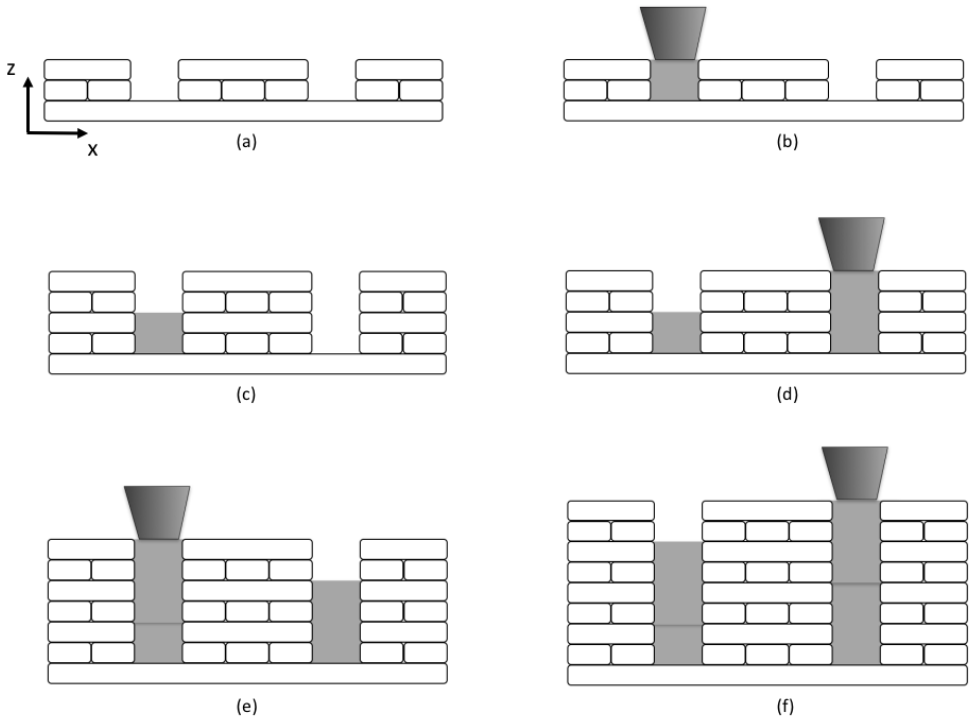


Figure 1. Illustration of the z-pinning approach for EDAM.

In addition to the spacing of pins throughout the part, a number of deposition parameters can influence the mechanical performance of the pinned structure [21]. A primary consideration is the ratio of the diameter of the hole to the diameter of the printing nozzle (D_H/D_N). If the diameter ratio is too high, the extruded material will coil at the bottom of the hole, creating multiple defects. If the ratio is too low, it is unlikely that the extruded material will reach the bottom of the hole. Likewise, the ratio of the length of the pin to the diameter of the hole (L_P/D_H) is also critical. A longer pin would provide more continuous material, fewer defects, and presumably additional strength. However, there is a limit to how deeply a pin could penetrate without introducing significant defects [21]. The volume of extruded pin compared to the theoretical volume of the corresponding hole (V_P/V_H) is another important ratio. Although it is difficult to exceed a "fill ratio" of 100 % in a solid structure, a sparse infill can allow excess pin material to infiltrate the surrounding structure, improving the pull-out strength of the pin through mechanical interlocking.

The z-pinning approach for EDAM was introduced in 2017 and is patent pending [22, 23]. It is very similar in a mechanical sense to the z-pinning technique introduced for composites in the 1970's to improve delamination toughness [4, 24-28]. Initial experiments with EDAM z-pinning showed promising results, increasing the toughness of PLA tensile samples by 100 % [22]. The improvements with fiber reinforced PLA were more dramatic, increasing z-strength by 3-5x and increasing the toughness by ~8x [29]. The current study extends these efforts, in conjunction with a submitted journal article [30], to directly compare the strength in the z-direction to the x-direction in order to quantify the degree of mechanical anisotropy.

2. EXPERIMENTATION

Vertical walls were printed on a desktop MakerGear (Fig 2) using unreinforced PLA (ECOMAX from 3DXTech, or "PLA") and a 15% carbon fiber reinforced PLA (CarbonX from 3DXTech, or "CF-PLA"). Two different sets of vertical walls were printed. The first set of walls used a rectilinear grid infill pattern in which the primary print direction of alternating layers was aligned with either the x- or y-axis (Fig 3a). The infill percentage of the rectilinear grid structure was either "solid" (~100 %) or "sparse" (35 % infill). The sparse infill grid was determined in previous studies to provide the appropriate diameter ratio for full penetration of 8-4 pins [21, 22, 29, 30]. The sparse grid structure contained either "no pins" or "8-4 pins" where the fill ratio (V_P/V_H) was equal to 120 %. The first set of walls were printed using both sets of materials: PLA was deposited at 210 °C, CF-PLA was deposited at 220 °C.

The second set of walls were printed as "solid" samples using CF-PLA at a temperature of 245 °C. The infill pattern on the second set of walls was a conventional 45/-45 raster (Fig 3b). The second set of walls were printed either without pins (95 % infill) or with 8-4 pins (90 % infill). The infill setting on the pinned samples was reduced slightly to avoid overfilling of the pin holes. The fill ratio of the pins deposited in the second set of walls had to be reduced significantly (fill ratio = 43 %) because the more solid structure did not have nearby cavities to absorb the overflow material.

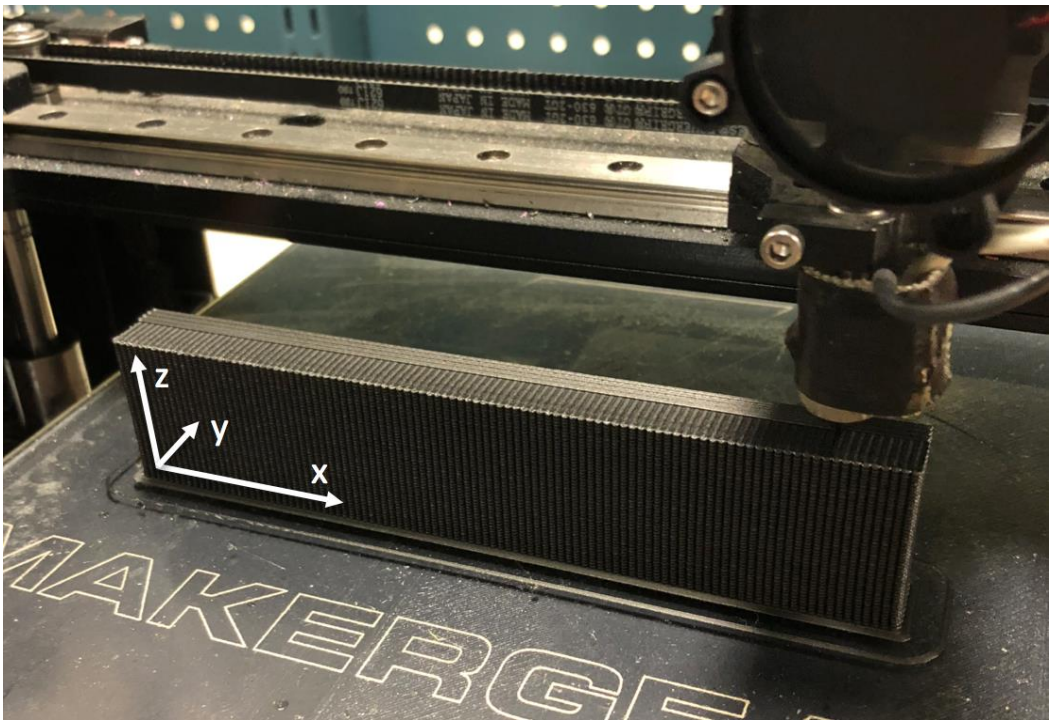


Figure 2. Vertical wall printed on a MakerGear with sample reference axes shown.

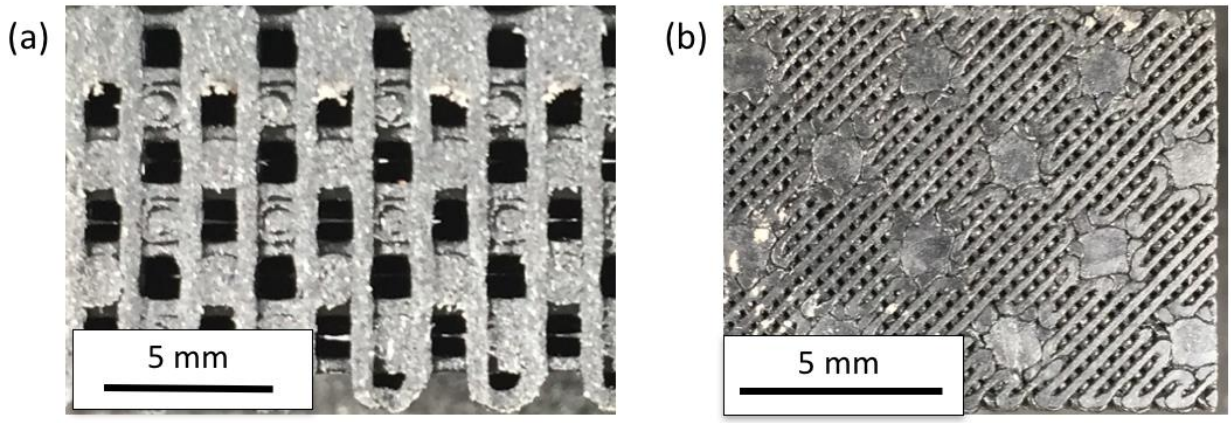


Figure 3. Pinned infill patterns for (a) rectilinear grid walls and (b) solid walls

Three tensile samples were cut from each wall for each test condition. The primary axis of the tensile sample was aligned with either the x- or z-axis (Fig 4) to obtain a direct comparison of strength in each direction in order to quantify mechanical anisotropy. The tensile samples were waterjet cut from the vertical walls according to the dimensions shown in Figure 5. Note that the shape of the tensile samples were slightly different between the two sample groups because several of the tensile samples in the first group were failing close to the transition section. Also note that each test condition using the rectilinear grid infill (first set of walls) had six repeat samples, whereas the second set of walls only had three repeat samples per test condition. The rectilinear grid samples were 12.7 mm thick as printed and each sample cross section contained two rows of A/B pins. The second set of walls were originally printed with a 20 mm thickness and had to be machined to 13.5 mm thickness to accommodate the tensile machine grip opening. Therefore, the second set of vertical walls contained two rows of A pins and only one row of B pins across the gauge section. Both sets of samples were dried in a vacuum oven at 50 °C for at least eight hours prior to tensile testing on an MTS servo-hydraulic test system (110 kN load cell, strain rate 3 mm/min).

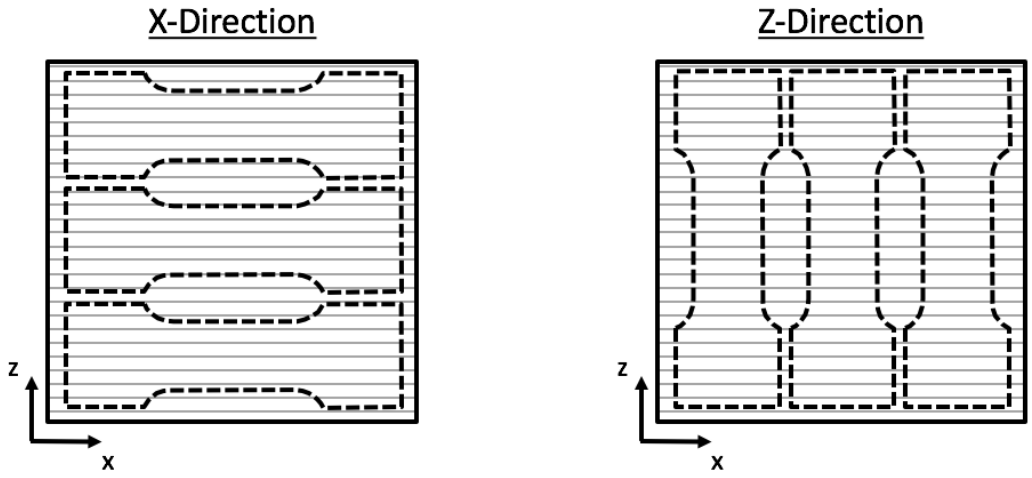


Figure 4. Orientation of tensile samples cut from vertical walls.

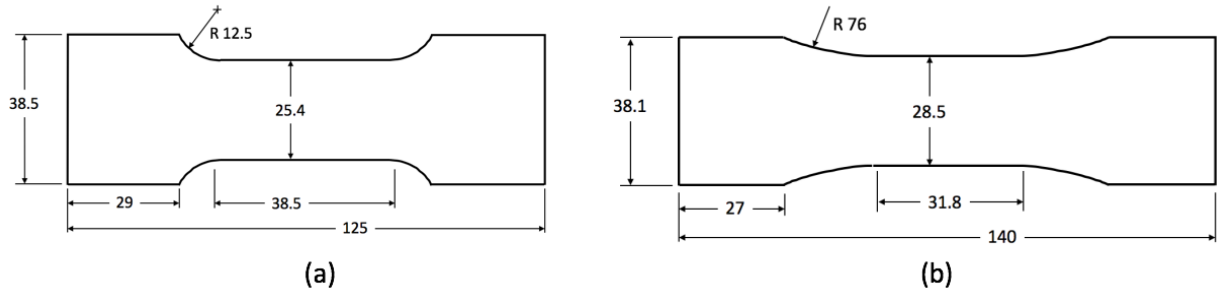


Figure 5. Tensile sample dimensions for (a) rectilinear grid samples and (b) solid infill samples. Dimensions are in mm.

3. RESULTS

The results of tensile testing of both sets of vertical walls are shown below for PLA and CF-PLA material sets. The first section compares the results of tensile testing directly while the second section considers the mechanical performance normalized by mass.

3.1 Tensile Test Results

Figure 6 shows the average ultimate tensile strength of PLA samples using the rectilinear grid infill pattern. Each data set directly compares the strength in the primary extrusion direction (x-axis) to the strength in the build direction (z-axis). The "Solid Grid" sample without pins demonstrates a loss in strength of ~33 % in the z-direction. Although the absolute values are low by comparison, the degree of mechanical anisotropy is very much on par with results reported by others for neat PLA [3, 4]. As expected, the sparse structure without pins loses considerable

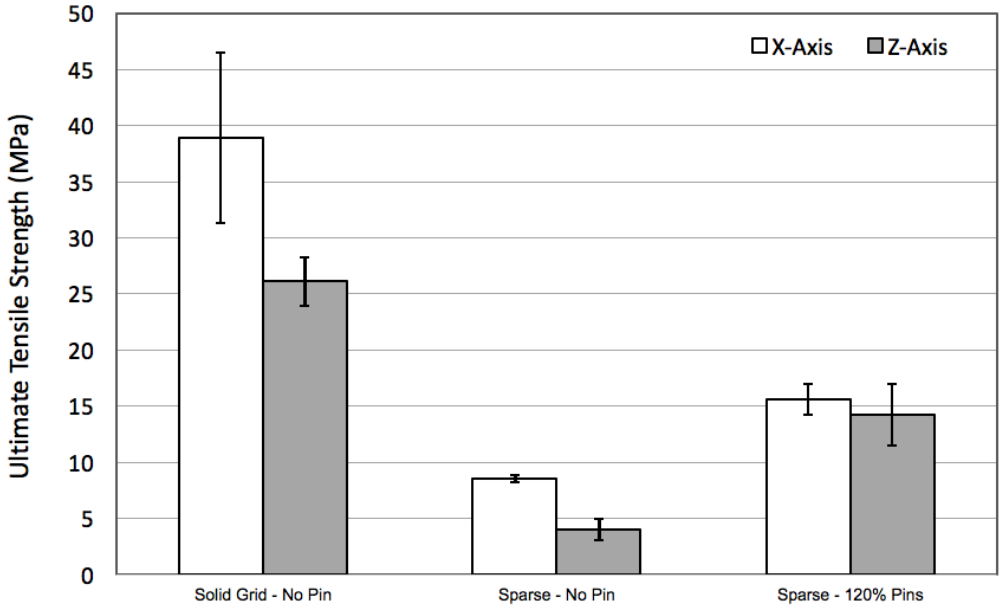


Figure 6. Ultimate tensile strength of PLA samples.

strength in both directions. Of particular interest, however, is the marked improvement in z-strength for the sparse structure. The addition of 8-4 pins with a fill ratio of 120 % was able to increase the z-direction strength by a factor of 3.5x and shows only ~10 % drop in strength compared to the primary x-direction. When considering the scatter in data for the pinned samples, there is no statistically significant difference in strength between the x- and z-directions – indicating that z-pins are able to produce a quasi-isotropic material.

Figure 7 shows a similar strength comparison for CF-PLA samples from both sets of walls. Samples from the second set of walls have higher strength in general, which could result from the either the higher deposition temperature or the infill raster pattern. Both sets of solid samples without pins show a decrease in strength in the z-direction between 30 % and 40 %, which corresponds well to previous studies with fiber reinforced PLA [4]. Similar to the results with neat PLA, the addition of pins to the sparse structure shows a dramatic increase in z-direction strength (>3x), although there is still a 30% decrease in strength compared to the x-axis. Adding pins to the solid structure did not increase the z-direction strength compared to the solid wall counterpart without pins. This could be due to the low fill ratio of the pins in the solid wall (43 %) or the increase in layer time (~30 %) to accommodate placement of the pins.

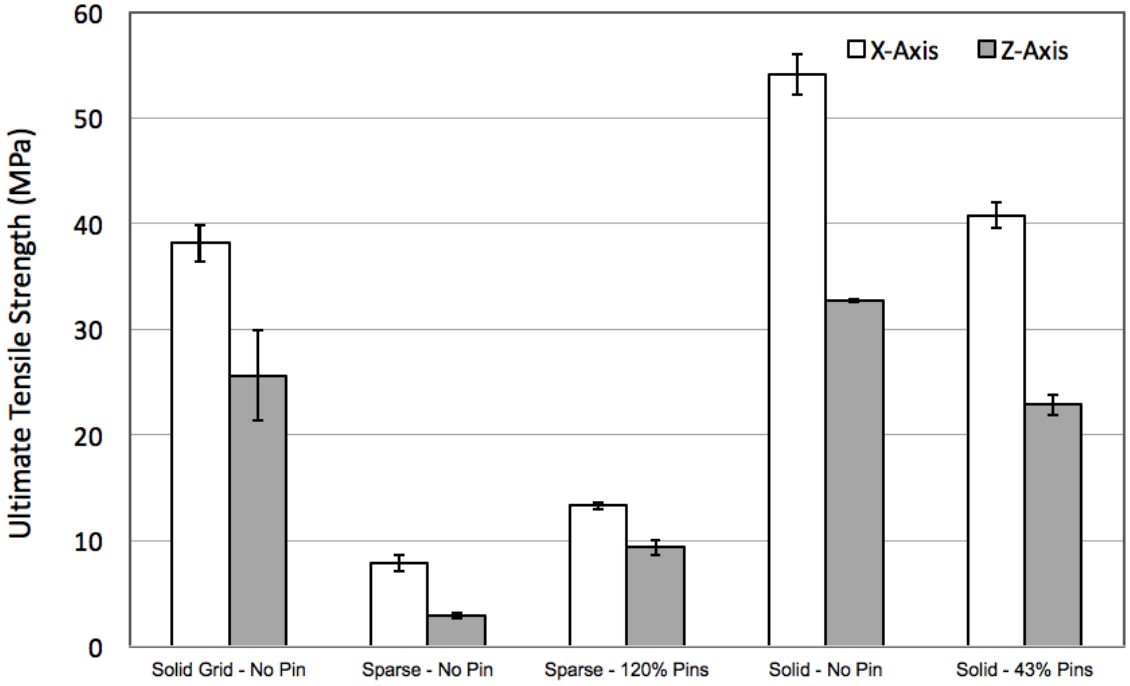


Figure 7. Ultimate tensile strength of CF-PLA samples.

Figures 8-10 compare the fracture surfaces for samples with and without z-pins. In each case, the left-most sample shows a very flat fracture surface without pins, indicating that there was very little deflection of the failure front as it moved through the sample. By comparison, the pinned samples have a tortuous fracture surface when tested in either the x-direction (b) or the z-direction (c). This may indicate that the crack propagation front was forced to deflect parallel to the load direction when a pin was encountered, which should increase both the strength and toughness of the sample when managed properly.

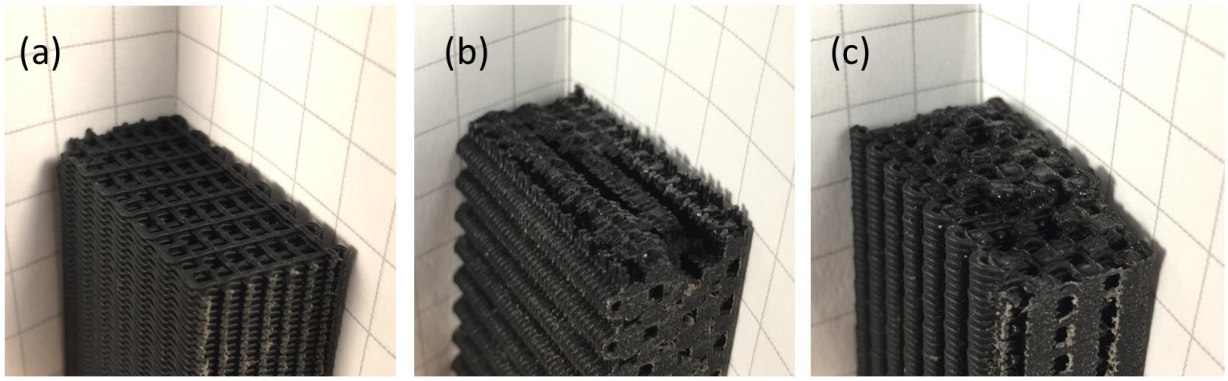


Figure 8. Fracture surface of PLA rectilinear grid samples: (a) z-direction, no pins (b) x-direction, 120 % pins (c) z-direction, 120 % pins. Note: square grid is 6.35 mm (1/4 inch).

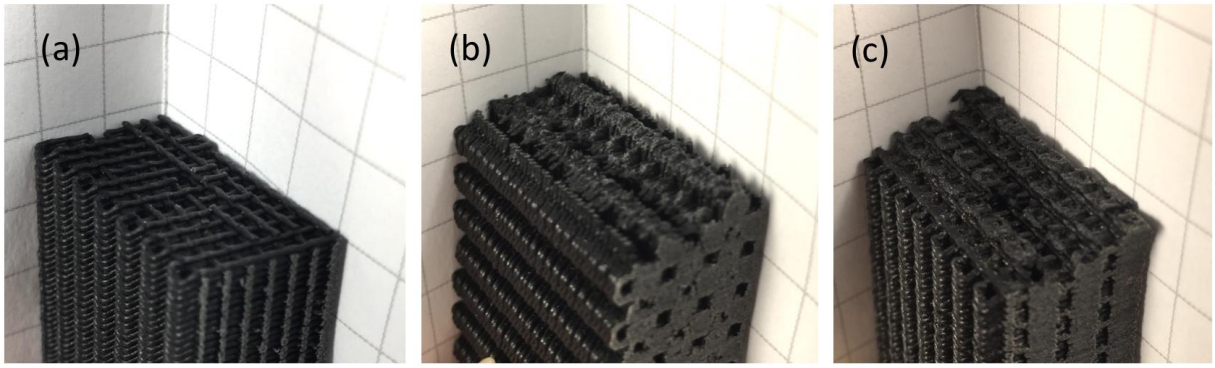


Figure 9. Fracture surface of CF-PLA rectilinear grid samples: (a) z-direction, no pins (b) x-direction, 120 % pins (c) z-direction, 120 % pins. Note: square grid is 6.35 mm (1/4 inch).

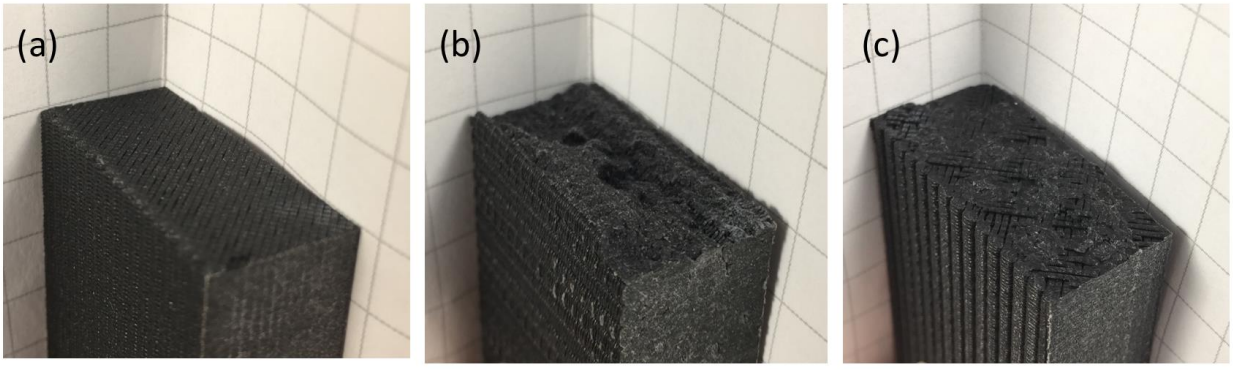


Figure 10. Fracture surface of CF-PLA solid infill samples: (a) z-direction, no pins (b) x-direction, 43 % pins (c) z-direction, 43 % pins. Note: square grid is 6.35 mm (1/4 inch).

3.2 Normalized Results

The rectilinear grid samples from the first set of walls was intentionally designed to have a large amount of internal void space to allow the pins to penetrate and mechanically interlock with the surrounding structure. However, a significant number of voids in a structure will obviously have a negative impact on the mechanical strength. Therefore, a more appropriate comparison between the different sample sets should take into account the mass differences. A similar approach for normalizing the mechanical strength based on the functional area was described in [30]. In the current paper, the mechanical performance is normalized by the average mass of the individual sample sets. As such, the mass of each sample sets was recorded in grams, and the ultimate tensile strength was divided by that number. Since the sample geometry was altered slightly between the first and second set of vertical walls (see Fig 5), the measured mass of the solid samples was reduced by 14 % to account for the corresponding increase in volume.

The mass-normalized strength values are shown in Figures 11 and 12 below. As expected, the relative strength of the sparse samples increased compared to that of the solid samples. However, since the mass of each sample set was nearly identical between x- and z-samples, there was no relative change to the degree of mechanical anisotropy.

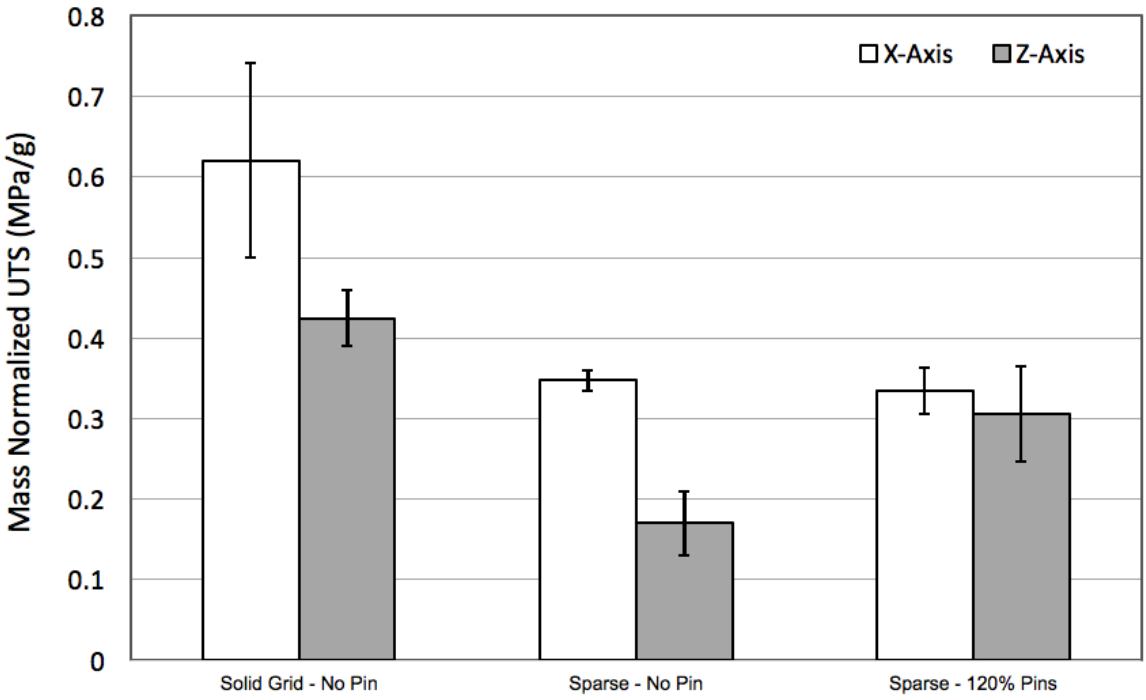


Figure 11. Mass normalized ultimate tensile strength (MPa/g) of PLA samples.

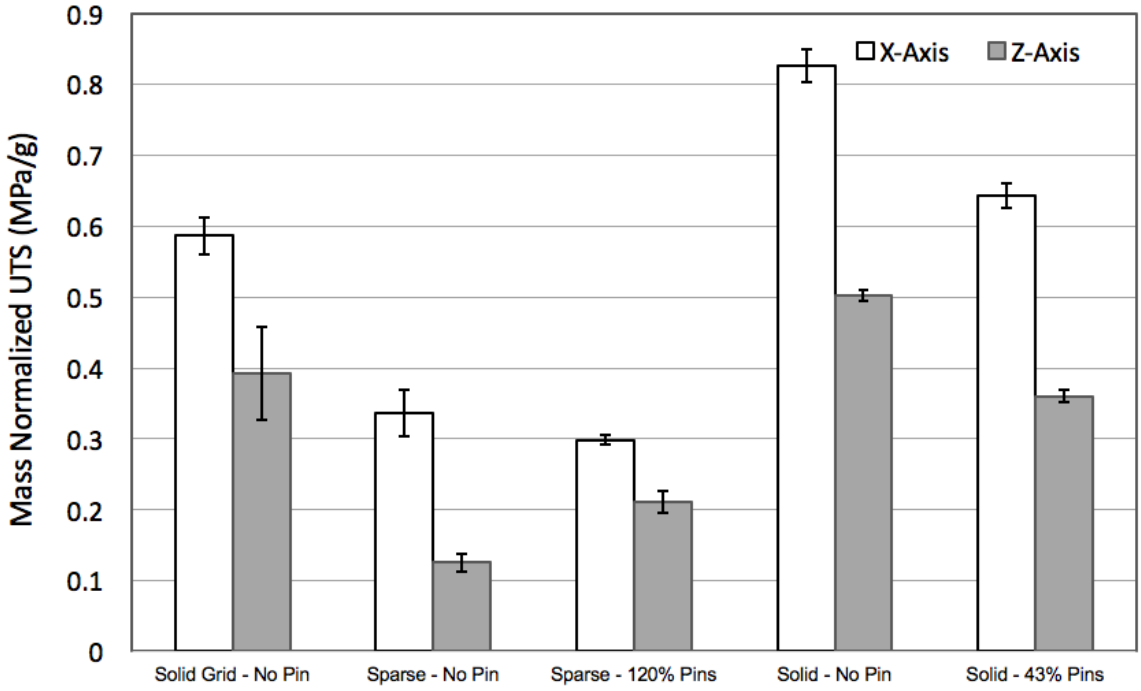


Figure 12. Mass normalized ultimate tensile strength (MPa/g) of CF-PLA samples.

4. CONCLUSIONS

A novel z-pinning approach for extrusion deposition additive manufacturing (EDAM) has been described and experimentally demonstrated for common 3D printing materials, PLA and carbon fiber reinforced PLA. This study compared the mechanical strength of samples cut from identical vertical walls in the x- and z-directions in order to directly quantify mechanical anisotropy. Z-pinning was shown to be an effective method for improving the z-directional strength of printed components, increasing strength by a factor of 3.5x and producing quasi-isotropic materials. There are a number of geometric and printing parameters that can affect the impact of the z-pinning method. In particular, z-pinning was shown to be particularly effective for sparse infill structures where mechanical interlocking can play a large role. Further development is needed to achieve similar gains for solid infill structures.

5. REFERENCES

[1] Torrado-Perez, A., D. Roberson, and R. Wicker. (2014) "Fracture Surface Analysis of 3D-Printed Tensile Specimens of Novel ABS-Based Materials". *Journal of Failure Analysis and Prevention* **14** pp. 343-353.

[2] Torrado, A.R., C.M. Shemelya, J.D. English, Y. Lin, R.B. Wicker, and D.A. Roberson. (2015) "Characterizing the Effect of Additives to ABS on the Mechanical Property

Anisotropy of Specimens Fabricated by Material Extrusion 3D Printing". *Additive Manufacturing* **6** pp. 16-29.
[3] Shaffer, S., K. Yang, J. Vargas, M. Di-Prima, and W. Voit. (2014) "On Reducing Anisotropy in 3D Printed Polymers Via Ionizing Radiation". *Polymer* **55** pp. 5969-5979.
[4] Ferreira, R.T.L., I.C. Amatte, T.A. Dutra, and D. Bürger. (2017) "Experimental Characterization and Micrography of 3D Printed Pla and Pla Reinforced with Short Carbon Fibers". *Composites Part B: Engineering* **124** pp. 88-100.
[5] Zhong, W., F. Li, Z. Zhang, L. Song, and Z. Li. (2001) "Short Fiber Reinforced Composites for Fused Deposition Modeling". *Materials Science and Engineering: A* **301** (2) pp. 125-130.
[6] Duty, C.E., V. Kunc, B. Compton, B. Post, D. Erdman, R. Smith, R. Lind, P. Lloyd, and L. Love. (2017) "Structure and Mechanical Behavior of Big Area Additive Manufacturing (BAAM) Materials". *Rapid Prototyping Journal* **23** (1).
[7] Eyercioglu, O., M. Aladag, and S. Sever. (2018) "Temperature Evaluation and Bonding Quality of Large Scale Additive Manufacturing Thin Wall Parts". *Sigma Journal of Engineering and Natural Sciences* **36** (3) pp. 645-654.
[8] Turner, B., R. Strong, and S. Gold. (2014) "A Review of Melt Extrusion Additive Manufacturing Processes: I. Process Design and Modeling". *Rapid Prototyping Journal* **20** (3) pp. 192-204.
[9] Sun, Q., G.M. Rizvi, C.T. Bellehumeur, and P. Gu. (2008) "Effect of Processing Conditions on the Bonding Quality of FDM Polymer Filaments". *Rapid Prototyping Journal* **14** (2) pp. 72-80.
[10] Rodriguez, J.F., J.P. Thomas, and J.E. Renaud. (2003) "Mechanical Behavior of Acrylonitrile Butadiene Styrene Fused Deposition Materials Modeling". *Rapid Prototyping Journal* **9** (4) pp. 219-230.
[11] Kishore, V., C. Ajinjeru, A. Nycz, B. Post, J. Lindahl, V. Kunc, and C. Duty. (2016) "Infrared Preheating to Improve Interlayer Strength of Big Area Additive Manufacturing (BAAM) Components". *Additive Manufacturing*.
[12] Ravi, A., *A Study on an in-Process Laser Localized Pre-Deposition Heating Approach to Reducing Fdm Part Anisotropy*. 2016, Arizona State University.
[13] Ravi, A., A. Deshpande, and K. Hsu. "An in-Process Laser Localized Pre-Deposition Heating Approach to Inter-Layer Bond Strengthening in Extrusion Based Polymer Additive Manufacturing." 2016.
[14] Partain, S., *Fused Deposition Modeling with Localized Pre-Deposition Heating Using Forced Air*. 2007, Montana State University.
[15] Sweeney, C.B., B.A. Lackey, M.J. Pospisil, T.C. Achee, V.K. Hicks, A.G. Moran, B.R. Teipel, M.A. Saed, and M.J. Green. (2017) "Welding of 3d-Printed Carbon Nanotube–Polymer Composites by Locally Induced Microwave Heating". *Science Advances* **3** (6).
[16] Adams, J.J., E.B. Duoss, T.F. Malkowski, M.J. Motala, B.Y. Ahn, R.G. Nuzzo, J.T. Bernhard, and J.A. Lewis. (2011) "Conformal Printing of Electrically Small Antennas on Three-Dimensional Surfaces". *Advanced Materials* **23** (11) pp. 1335-1340.
[17] Chakraborty, D., B. Aneesh Reddy, and A. Roy Choudhury. (2008) "Extruder Path Generation for Curved Layer Fused Deposition Modeling". *Computer-Aided Design* **40** (2) pp. 235-243.
[18] Khurana, J., T.W. Simpson, and M. Frecker. Structurally Intelligent 3D Layer Generation for Active Z-Printing." in Solid Freeform Fabrication Symposium. 2018. Austin, TX.

[19] Kubalak, J., C. Mansfield, T. Pesek, Z. Snow, E. Cottiss, O. Ebeling-Koning, M. Price, M. Traverso, L. Tichnell, C.B. Williams, and A. Wicks. "Design and Realization of a 6 Degree of Freedom Robotic Extrusion Platform." in *Solid Freeform Fabricatin Symposium*. 2016. Austin, TX.

[20] Kubalak, J.R., A.L. Wicks, and C.B. Williams. (2018) "Using Multi-Axis Material Extrusion to Improve Mechanical Properties through Surface Reinforcement". *Virtual and Physical Prototyping* **13** (1) pp. 32-38.

[21] Kim, S., T. Smith, J. Failla, J. Lindahl, V. Kunc, and C. Duty. (2018) "Parametric Analysis on Vertical Pins for Strengthening Extrusion-Based Printed Parts" *SAMPE 2018.* Long Beach, CA. May 21-24, 2018

[22] Duty, C., J. Failla, S. Kim, J. Lindahl, B. Post, L. Love, and V. Kunc. (2017) "Reducing Mechanical Anisotropy in Extrusion-Based Printed Parts" *Solid Freeform Fabrication Symposium.* Austin, TX. August 2017

[23] Duty, C., J. Failla, V. Kunc, J. Lindahl, B. Post, L. Love, and S. Kim (2018) "Z Layer Improvement Using Liquid Nails Method." U.P. Application 15/965,106 filed April 27, 2018.

[24] Boyce, J.S., G.A. Freitas, C.L. Magee, T.M. Fusco, J.J. Harris, and E. Kunkle (1998) "Ultrasonic Fastening System and Method." filed 1998.

[25] Freitas, G.A., C.L. Magee, P. Dardzinski, and T.M. Fusco. (1994) "Fibre Insertion Process for Improved Damage Tolerance in Aircraft Laminates." *Journal of Advanced Materials* **25** pp. 36-43.

[26] Krasnov, V., V. Kuznetsov, and A. Maksokov. (1987) "Automated Method of Transverse Reinforcement of Composites by Short Fibres.". *Mechanika Kompozitnykh Materialov* **3** pp. 449-504.

[27] Mouritz, A.P. (2007) "Review of Z-Pinned Composite Laminates". *Composites: Part A* **38** pp. 2383-2397.

[28] Tomashevskii, V.T., S.Y. Sitnikov, V.N. Shalgin, and V.S. Yakovlev. (1989) "A Method of Calculating Technical Regimes of Transversal Reinforcement of Composites with Short-Fibre Microparticles.". *Mekhanika Kompozitnykh Materialov*.

[29] Duty, C., J. Failla, S. Kim, T. Smith, J. Lindahl, A. Roschli, B. Post, L. Love, and V. Kunc. Z-Pinning Approach for Reducing Mechanical Anisotropy of 3d Printed Parts." in *Solid Freeform Fabrication Symposium*. 2018. Austin, TX.

[30] Duty, C., J. Failla, S. Kim, T. Smith, J. Lindahl, and V. Kunc. (2019) "Z-Pinning Approach for 3d Printing Mechanically Isotropic Materials". *Additive Manufacturing* (submitted).